Electron Emission from Slow Hollow Atoms at a Clean Metal Surface

H. Kurz, K. Töglhofer, HP. Winter, and F. Aumayr
Institut für Allgemeine Physik, Technische Universität Wien, Wiedner Hauptstrasse 8-10, A-1040 Wien, Austria

R. Mann
Gesellschaft für Schwerionenforschung, Postfach 110552, W-6100 Darmstadt 11, Germany
(Received 27 April 1992)

For impact of slow multicharged N, Ne, Ar, and I ions on clean polycrystalline gold (impact velocity $1\times10^4 < v_p < 15\times10^4$ m/s), for the first time the statistics of the resulting electron emission have been determined, from which rather precise total electron yields have been derived. From the impact-velocity dependences of yields and the shapes of electron multiplicities two different contributions to electron emission are identified, one probably being due to autoionization before surface impact and the other due to faster autoionization just at the surface or already inside the solid.

PACS numbers: 79.20.Nc, 79.20.Rf

Multicharged ions (MCI, Z^{q+}) can capture electrons resonantly from states near the Fermi edge of a metal surface within a critical distance d_c which depends on the wave-function overlap of the surface density of states with empty projectile states. Consequently, d_c increases for higher projectile charge q and/or lower surface work function W_ϕ. Once within this critical range, a slow MCI with impact velocity $v_p \ll 1$ a.u. will be rapidly further neutralized according to a characteristic time t_n related to the Fermi velocity v_F, which for metals is of the order of 1 a.u. [1]. Such developing multiply excited ("hollow") atoms become subject to resonant ionization (RI) as well as autoionization (AI), which together with the ongoing resonant neutralization (RN) determine the projectile's electronic population until it hits the surface [2,3]. As a result of AI, slow electrons should be emitted from projectiles [4] more efficiently the lower the impact velocity [5]. What exactly happens to electrons still bound to a projectile in highly excited states at the moment of surface impact could not be studied in detail so far, either theoretically or experimentally. Sufficiently slow projectiles may be reflected in the repulsive planar surface potential [3], whereas faster ones will penetrate into the solid to undergo various deexcitation processes until their complete neutralization and stopping. This scenario has been studied by analyzing the related total electron emission yields [4–6] and energy distributions [3,6–9], charge-state composition of scattered projectiles [10,11], and emission of soft x rays [3,12,13]. The electron energy distributions are dominated by low-energy continua [9,14] ($E_e < 30$ eV); smaller contributions from fast Auger electrons, also observed [3,7–9,14], originate mainly from below the surface [7]. Several reviews on the slow-MCI–surface interaction [3,15] and related semiclassical [2] and classical [16] theories have recently been published, as well as quantum-mechanical calculations on the involved RN [17] and AI processes [18].

In this paper we deal with the first leg of an MCI's journey from its initial RN until the close contact with a clean metal surface, by studying emission of slow ($E_e \leq 60$ eV) electrons during the projectile flight time $t_f = d_c/v_p$ toward the surface, to shed more light on the sequence of formation and decay of the transiently produced, multiply excited atoms. By means of a novel method [19] we determined the electron emission statistics (ES), i.e., the probabilities W_n for emission of $n = 0,1,2,\ldots$ electrons per impinging MCI. This method offers distinct advantages over the common measurement of total electron yields from currents of primary ions and emitted electrons [5,6], namely, a much higher sensitivity, which reduces the required primary MCI current dramatically, rather precise absolute electron yields directly available from the essentially relative ES measurements, and, most notably, completely new information related to the electron emission multiplicity of such processes.

A recoil ion source [20] pumped by fast (3–11 MeV/amu) heavy-ion beams from the GSI UNILAC accelerator delivered MCI fluxes of, e.g., 100/s for Ar^{16+} or 10^4/s for Ar^{10+} at the target surface. After their extraction with several hundred volts and charge-to-mass separation in a 180° magnet, the recoil ions ($N^{q+}/q \leq 6$, $Ne^{q+}/q \leq 10$, $Ar^{q+}/q \leq 16$, $I^{q+}/q \leq 25$) were guided toward our ES detector [21]. Their small initial kinetic-energy spread permitted deceleration to rather low nominal target impact energies $E \geq (2 \pm 1)q$ eV by means of a four-cylinder lens in front of the target surface. The final part of the MCI beam line and the ES detector assembly including the target (atomically clean polycrystalline gold, sputter cleaned by means of a built-in Ar^+-ion gun) were kept in UHV at a base pressure of typically some 10^{-8} Pa during all measurements. ES were determined for impact of various MCI species such that a fountain-type cylindrical electrode arrangement [21] forced all electrons ejected from the target surface with energies of $E_e \leq 60$ eV into the full 2π solid angle toward a surface barrier detector biased at +25 kV with respect to the target. From the resulting pulse height spectrum

we derived the emission probabilities W_n, which in their entirety constitute the corresponding ES [19].

Raw ES data, as shown in Fig. 1 for 100-eV Ar^{q+}, were evaluated according to the procedure described in Ref. [22] to obtain the emission probabilities W_n. The apparent degradation of detector resolution with increasing projectile charge, which is due to backscattering of individual electrons from the detector surface, has been taken into account quantitatively [22]. The probability W_0, which obviously cannot be directly determined with our method, may safely be neglected for total yields $\gamma \geq 5$. Typical examples for total electron yields γ (accuracy typically $\pm 3\%$ [19]) and ES are shown for Ar^{q+} ions of different impact velocities in Figs. 2 and 3, respectively. Both the actual MCI impact velocity and the influence of target surface roughness on the electron yields will be discussed later on.

Figure 2 shows that with increasing v_p the electron yields first decrease gradually and then level off towards an apparently velocity-independent value γ_∞. The velocity-dependent part of the yield $(\gamma - \gamma_\infty)$ originates presumably from AI of the projectiles (i.e., the hollow atoms) on their way toward the surface. Calculating d_c according to Ref. [2], which gives almost the same results as a corresponding classical treatment [16], and taking $W_\phi = 5.1$ eV for clean gold [1], we obtain (atomic units are used unless otherwise stated)

$$d_c = \frac{1}{2W_\phi}\sqrt{8q+2} \approx 0.4\sqrt{q}\ \text{nm for } q \gg 1 . \quad (1)$$

At the lowest impact energies, Eq. (1) leads to typical projectile flight times $t_f \approx 10^{-13}$ s, which by considering the velocity dependence of γ (cf. Fig. 2) results in "mean apparent AI rates" of typically 10^{14} s^{-1}. If successive electron emission events would involve equal AI rates, $\gamma - \gamma_\infty$ should scale like $1/v_p$. However, if the rates for successive AI events decrease, a flatter velocity dependence $\gamma - \gamma_\infty \sim v_p^{-\alpha}$ (with $0 < \alpha < 1$) will result. Indeed, we find the relation

$$\gamma \approx \text{const} \times v_p^{-0.5} + \gamma_\infty , \quad (2)$$

fitting the measured total yields (cf. Fig. 2) rather well.

We may explain such a presumed decrease of involved apparent AI rates as follows. On its way toward the surface, the particle becomes subject to both RI and AI, whereby only the latter can cause the observed electron emission. It has been shown [3] that because of "screen-

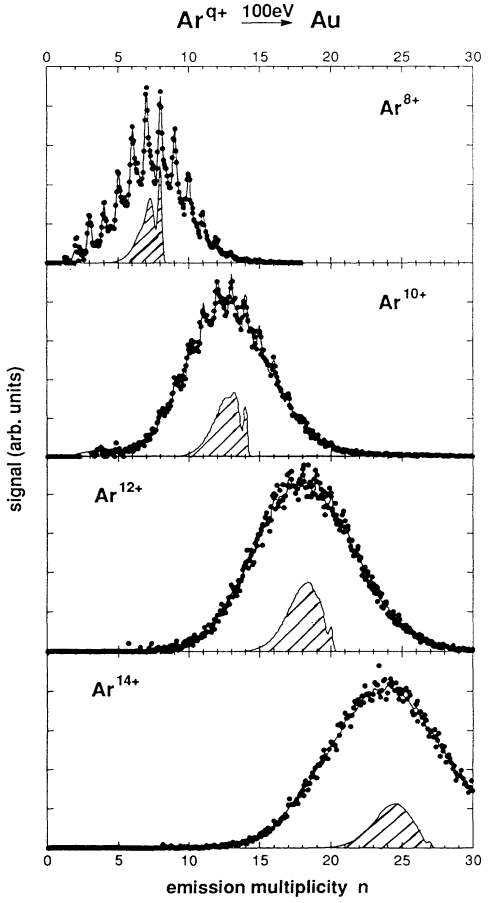

FIG. 1. Measured pulse height spectra for impact of 100-eV Ar^{q+} in different charge states on clean polycrystalline gold. Measured data were fitted (solid line) for deconvolution into individual multiplicities. The hatched insets show the energy deposition distribution for the respective most probable number of emitted electrons.

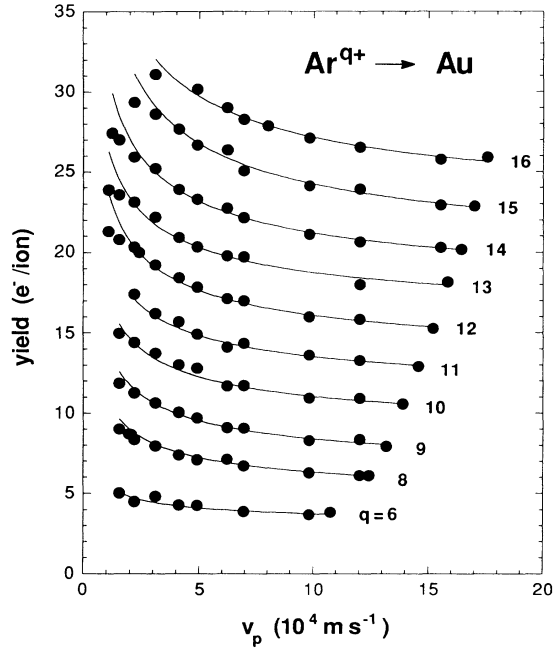

FIG. 2. Total electron yields vs impact velocity as derived from the measured ES, for impact of Ar^{q+} on clean polycrystalline gold ($q = 6$–16). The solid lines are fits according to Eq. (2). Note the clear deviation from these fits at low v_p which is ascribed to image-charge acceleration of projectiles.

ing dynamics" RN populates the projectile Rydberg states with increasingly lower principal quantum numbers during the particle's approach toward the surface. Consequently, the resulting apparent AI rates should decrease as well with decreasing distance from the surface, because of the decreasing probability to occupy empty lower projectile states which permit AI transitions just into vacuum (transitions that would involve the relatively largest rates [18]). In addition, the competing RI processes become more efficient closer to the surface [2].

Furthermore, at the lowest impact velocities Fig. 2 shows a deviation from the γ vs v_p dependence as described by Eq. (2), which we may relate to a gain in projectile impact energy because of image-charge attraction [2,7,11,23]. Until its first RN at the distance d_c [cf. Eq. (1)], an ion Z^{q+} has gained a kinetic energy

$$E_{q,\mathrm{im}} = q^2/4d_c \cong 0.9q^{3/2}\,\mathrm{eV}\,. \tag{3a}$$

However, fitting a $q^{3/2}$ dependence to the available experimental data [11] for Ar^{q+} ($q \leq 6$) results in

$$E_{q,\mathrm{im}} \cong 1.2q^{3/2}\,\mathrm{eV}\,. \tag{3b}$$

The larger factor in Eq. (3b) can be fully accounted for by considering the further projectile acceleration inside d_c with a stepwise decreasing ion charge [2]. Apparently it makes no sense to aim for lower impact velocities than the absolute limit [11] set by Eq. (3b) (e.g., ca. 77 eV or 1.9×10^4 m/s for Ar^{16+}) irrespective of the chosen impact geometry.

Considering now the observed emission statistics it is easily demonstrated that the ES should follow a Poissonian distribution if the slow electron emission would result from a number of mutually independent, equally fast AI processes. As an example, Fig. 3 shows ES for Ar^{12+} at three different impact energies. Gaussian distributions fit these ES very well, whereas Poissonian distributions for the same mean values γ are clearly too broad, as indicated for the 500-eV case. This implies that the processes responsible for electron emission involve less randomness than one had to expect for fully independent emission of the individual electrons. However, the velocity-independent contribution γ_∞ cannot result only from "peeling off" the $\leq q$ electrons still bound within highly excited states, when the projectile reaches the surface [2], because for higher ion charge states γ_∞ clearly surpasses q [$\gamma_\infty \approx 12$ for $q=12$, but $\gamma_\infty \approx 21$ for $q=16$; cf. Fig. 2 and Eqs. (4) below]. Kinetic electron emission does not yield more than 0.5 electron/ion at $v_p \leq 2\times10^5$ m/s [21]. We therefore propose some "ultimate," very fast autoionization and/or Auger neutralization (AN) processes [6] occurring rather close to or already beyond the surface as soon as the still populated highly excited projectile states overlap completely with the filled metal states. These processes may be fast enough to stay practically independent of the MCI impact velocity within its limits considered here.

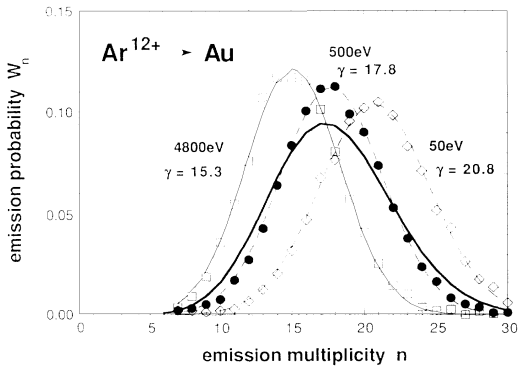

FIG. 3. Electron emission statistics (ES) as derived by unfolding the raw pulse height spectra (cf. Fig. 1) for impact of Ar^{12+} with different impact energies on clean polycrystalline gold. The dashed lines are fitted Gaussian distributions. For the 500-eV data a Poissonian (solid line) with appropriate mean value γ has been added (for further explanations see text).

For Ar^{q+} projectiles ($q=8$–16) we found the following linear dependences (least-squares fits) for both γ and γ_∞ versus ion charge q:

$$\begin{aligned} &\gamma = 2.97q - 15.4 \quad (\text{for } E_{\mathrm{kin}} = 100\,\mathrm{eV})\,,\\ &\gamma = 2.67q - 15.0 \quad (\text{for } E_{\mathrm{kin}} = 1\,\mathrm{keV})\,,\\ &\gamma_\infty = 2.10q - 12.9\,. \end{aligned} \tag{4}$$

Earlier studies [4,5,8] of MCI impact-related total electron yields showed for Ar^{q+} ($q \leq 8$) the total yields γ being directly proportional to the MCI's total potential energy, but for $q \geq 9$ the onset of inner-shell vacancy formation in the course of RN caused a marked leveling off from this behavior. According to Eqs. (4) the linear increase of the contributions γ_∞ with q, which we have just ascribed to some ultimate AN and/or AI, points to a direct proportionality of the yield increments with the number ($\approx q$) of electrons still carried in Rydberg states of the projectile [2] at its surface impact.

The arguments presented above are supported by our results for other projectile species, in particular N^{6+} and I^{25+}. For N^{6+} we found almost no variation of the total electron yield ($\gamma \approx 5$) with v_p, which in the light of the above discussion points to a complete domination of RI over AI and thus a rather effective suppression of the electron yield contribution ($\gamma - \gamma_\infty$) during the approach of N^{6+} toward the surface. Consequently, the corresponding total electron yield seems to be exclusively due to the above-introduced ultimate AI and/or AN processes at and/or below the surface. This remarkable result strongly suggests a reassessment of models both for the filling of electronic states prior to the inner-shell vacancy-related fast Auger electron emission [7–9] and for the AI processes assumed responsible for the slow electron emission [18].

On the other hand, results for the impact of 200-eV

I^{25+} ($\gamma=70$) provide an extreme example for pure potential emission, where up to $n=85$ electrons could be ejected by a single MCI. There, in contrast to N^{6+}, the AI seems to be much less inhibited by RI and the velocity-dependent contribution $(\gamma-\gamma_\infty)\approx 40$ electrons/ion appears as a major part of the total yield. RN of the Ni-like I^{25+} ions cannot produce transient inner-shell vacancies; this seems to increase electron emission by the AI processes during the particle's approach toward the surface.

As a general result, roughness of the Au surface can influence the total electron yield only via the γ vs v_p dependence, but cannot modify the shape of a power law like Eq. (2).

In conclusion, we introduced a new way to investigate slow electron emission due to slow multicharged ion impact on a clean metal surface by measuring the resulting electron emission statistics which also deliver rather precise total electron yields. By combining this technique with a fast heavy-ion-pumped recoil MCI source, very low impact energies (probably only limited by the apparent image-charge acceleration of projectile ions) could be achieved and quite small ion fluxes were fully sufficient for precise γ measurements.

The observed impact-energy dependences of electron yields and emission statistics suggest that the former are probably composed of two parts. The first one is generated during the projectile's flight to the surface and increases with decreasing impact velocity in a way which reflects a competition between autoionization and resonance ionization of the hollow projectile atoms being formed near the surface. The result of this competition should depend rather sensibly on both the surface density of states and the electronic structure of neutralized projectiles.

A second, apparently impact-velocity-independent contribution is ascribed to rather fast multiple autoionization and/or Auger neutralization processes occurring just upon surface impact or within the first few monolayers of the solid, and was found to increase linearly with the number of electrons still bound within highly excited projectile states at the moment of impact.

The present results provide new insights to processes induced by slow-multicharged-ion–metal-surface interaction and thus are of interest for the closely related fast Auger electron and x-ray photon emission phenomena. Further details will probably be learned from ongoing comparative studies with various MCI species (particularly at the lowest attainable ion energies) and (preferably monocrystalline flat) target surfaces.

The authors are indebted to the accelerator staff of GSI for their good collaboration in providing the fast heavy-ion beams. Work has been supported by Austrian Fonds zur Forderung der wissenschaftlichen Forschung under Project No. P8315TEC, and by Kommission zur Koordination der Kernfusionsforschung at the Austrian Academy of Sciences.

[1] N. W. Ashcroft and N. D. Mermin, *Solid State Physics* (CBS Publ. Asia Ltd., Philadelphia, 1976).
[2] J. Burgdörfer, P. Lerner, and F. W. Meyer, Phys. Rev. A **44**, 5674 (1991).
[3] H. J. Andrä *et al.*, in *Electronic and Atomic Collisions*, edited by W. R. MacGillivray, I. E. McCarty, and M. C. Standage, IOP Conference Proceedings (Institute of Physics, Bristol, 1992), p. 89.
[4] U. A. Arifov, L. M. Kishinevskii, E. S. Mukhamadiev, and E. S. Parilis, Zh. Tekh. Fiz. **43**, 181 (1973) [Sov. Phys. Tech. Phys. **18**, 118 (1973)].
[5] M. Delaunay, M. Fehringer, R. Geller, D. Hitz, P. Varga, and HP. Winter, Phys. Rev. B **35**, 4232 (1987).
[6] H. D. Hagstrum, Phys. Rev. **96**, 325 (1954); **96**, 336 (1954).
[7] P. A. Zeijlmans van Emmichoven, C. C. Havener, and F. W. Meyer, Phys. Rev. A **43**, 1404 (1991); F. W. Meyer, S. H. Overbury, C. C. Havener, P. A. Zeijlmans v. Emmichoven, J. Burgdörfer, and D. M. Zehner, Phys. Rev. A **44**, 7214 (1991).
[8] S. T. de Zwart, Ph.D. thesis, University of Groningen, 1987 (unpublished); S. T. de Zwart, A. G. Drentje, A. L. Boers, and R. Morgenstern, Surf. Sci. **217**, 298 (1989); L. Folkerts and R. Morgenstern, Europhys. Lett. **13**, 377 (1990).
[9] M. Delaunay, M. Fehringer, R. Geller, P. Varga, and HP. Winter, Europhys. Lett. **4**, 377 (1987).
[10] S. T. de Zwart, T. Fried, U. Jellen, A. L. Boers, and A. G. Drentje, J. Phys. B **18**, L623 (1985).
[11] H. Winter, Europhys. Lett. **18**, 207 (1992).
[12] E. D. Donets, Nucl. Instrum. Methods Phys. Res., Sect. B **9**, 522 (1985).
[13] J. P. Briand, L. de Billy, P. Charles, S. Essabaa, P. Briand, R. Geller, J. P. Desclaux, S. Bliman, and C. Ristori, Phys. Rev. Lett. **65**, 159 (1990); Phys. Rev. A **43**, 565 (1991); M. Schulz, C. L. Cocke, S. Hagmann, M. Stöckli, and H. Schmidt-Böcking, Phys. Rev. A **44**, 1653 (1991).
[14] J. W. McDonald, D. Schneider, M. W. Clark, and D. Dewitt, Phys. Rev. Lett. **68**, 2297 (1992).
[15] P. Varga, Comments At. Mol. Phys. **23**, 111 (1989); HP. Winter, Z. Phys. D **21**, S129 (1991).
[16] J. N. Bardsley and B. M. Penetrante, Comments At. Mol. Phys. **27**, 43 (1991).
[17] U. Wille, Z. Phys. D **21**, S353 (1991); Phys. Rev. A **45**, 3004 (1992).
[18] N. Vaeck and J. E. Hansen, J. Phys. B **24**, L469 (1991).
[19] G. Lakits, F. Aumayr, and HP. Winter, Rev. Sci. Instrum. **60**, 3151 (1989).
[20] R. Mann, Z. Phys. D **3**, 85 (1986).
[21] G. Lakits, F. Aumayr, M. Heim, and HP. Winter, Phys. Rev. A **42**, 5780 (1990); HP. Winter, F. Aumayr, and G. Lakits, Nucl. Instrum. Methods Phys. Res., Sect. B **58**, 301 (1991).
[22] F. Aumayr, G. Lakits, and HP. Winter, Appl. Surf. Sci. **47**, 139 (1991).
[23] F. W. Meyer, S. H. Overbury, C. C. Havener, P. A. Zeijlmans v. Emmichoven, and D. M. Zehner, Phys. Rev. Lett. **67**, 723 (1991).